Available online at www.sciencedirect.com
SCIENCE DIRECT®
Journal of Electron Spectroscopy and Related Phenomena 143 (2005) 51–64
JOURNAL OF ELECTRON SPECTROSCOPY and Related Phenomena
www.elsevier.com/locate/elspec

Theory of the near *K*-edge structure in electron energy loss spectroscopy

A.T. Paxton*

Atomistic Simulation Centre, Department of Physics and Astronomy, Queen's University, Belfast BT7 1NN, UK

Received 11 November 2003; received in revised form 19 May 2004; accepted 19 May 2004
Available online 9 December 2004

Abstract

Arguments are given that lead to a formalism for calculating near *K*-edge structure in electron energy loss spectroscopy (EELS). This is essentially a *one electron* picture, while many body effects may be introduced at different levels, such as the local density approximation to density functional theory or the GW approximation to the electron self-energy. Calculations are made within the all electron LMTO scheme in crystals with complex atomic and electronic structures, and these are compared with experiment.

Keywords: One-electron theory; Inelastic scattering; *K*-edge

1. Introduction

As is well known, there are features called *edges* in the electron energy loss spectra of solids that appear at energies beyond the low loss and valence electron regions. These are sharp increases in the inelastic scattering intensity due to excitations of the core electrons of the atoms in the specimen into unoccupied states in the conduction band or above the Fermi level. The absolute position of the edge is a measure of the smallest energy needed to eject a particular core electron into some unoccupied state. This must be thought of as the energy difference between the final and initial states of the specimen, since it is exactly this amount of energy that is lost from the electron beam. In view of the very low flux in a typical experiment, we may take it that the initial state is the quantum mechanical ground state; the final state features a core hole, the electron that occupied that state now belonging to the conduction band. In an independent electron picture we say that the energy loss is equal to the difference in *eigenvalues* of the (previously unoccupied) conduction band state and the core level. However this approach may neglect any rearrangement of the remaining electrons in the crystal due to the sudden appearance of the core hole. Strictly speaking this is a two-body problem if we wish to treat both the electron and hole on an equal footing. Such an approach is necessary in the discussion of valence electron spectra in which the electron and hole are rather close in energy and form a dynamically bound pair, or *exciton* [1]. However to describe core level spectroscopy it is sufficient to treat the effect of the core hole by the "switching on" of a static potential very suddenly as the fast electron strikes the specimen foil. This is known as the *sudden approximation*. The situation then reduces to a one electron problem as we shall see.

Of much greater interest than the threshold energy itself is the structure of the spectrum above the edge that becomes superimposed on the uniform decaying atomic background, due to the atomic and electronic structure of the material in the foil. At energies typically some tens of electron volts above the edge, the spectrum is usually oscillatory, and this *extended fine structure* gives detailed information about the local atomic environment of the atom that is excited by the incoming beam. The interpretation of this structure is rather well developed and will not be discussed here. At energies of just a few electron volts above the edge, one finds the *near edge structure*, whose details reflect the electronic structure of the specimen in the region of the foil around the excited

* Tel.: +44 2890 975328; fax: +44 2890 975359.
E-mail address: tony.paxton@qub.ac.uk.
URL: http://titus.phy.qub.ac.uk.

0368-2048/$ – see front matter © 2004 Elsevier B.V. All rights reserved.
doi:10.1016/j.elspec.2004.05.007

atom. By comparing detailed features of the experimental spectrum with known features of either standard specimens or those from calculations on ideal crystals EELS is used as a tool of very high spatial and energetic resolution to determine the local atomic and electronic structure of defects in crystals: grain boundaries, interfaces, precipitates and so on. A typical application is the measurement of the *white line* in transition metal $L_{2,3}$ edges in order to determine the local band filling [2]; or the determination of the oxidation state of ions at defects in ionic crystals [3]. The subject is now sufficiently far advanced that many articles have appeared that describe one or other aspect of the theory.

The intention here is to present the steps needed toward calculation of the near *K*-edge structure in the one electron approximation. Two approaches are described. The first is the theory of Bethe which is well known in electron microscopy and beautifully includes both elastic and inelastic scattering in a single formula. We present it here because a derivation is not easily found in the literature and we wish to find an expression for the scattered intensity in terms of the *dynamical form factor* which is often familiar in other contexts. The Bethe theory does not easily expose the point that the process should be describable in a one electron picture. We therefore obtain the one electron approximation to Bethe's formula again using a quite different approach due to Hedin. Our calculations are then made using a particular one electron form of the matrix elements, namely the local density approximation to density functional theory. However the theory of Hedin is easily extended to the case that the one electron potential is energy dependent and non-local and we give one example of such a calculation in NiO in which electron correlations are expected to be very strong.

We will confine ourselves to the discussion of *K*-edges which are those that arise from the excitations of s-electrons from the core; these are the only core states whose wavefunctions do not have multiplet structure. To discuss p, d and f core states requires us to go beyond the usual approximation that wavefunctions can be described in non-relativistic quantum mechanics by a single Slater determinant and this takes us beyond the scope of the present work. Fortunately there is a very good recent review of multiplet effects [4].

2. Calculation of the scattered intensity

In the sudden approximation, we expect the scattered intensity to be rendered in a *one electron* approximation. That does not preclude electron–electron interactions as in an *independent electron* approximation in which electrons are found in states whose energies are independent of the presence of other electrons. Instead each electron is said to see a potential that includes the effects all the other electrons; this potential need not be local or energy independent, although this is the case in density functional theory described below. In this section we will describe two approaches that begin in a many electron framework; each of which reduces to a formulation in terms of one electron matrix elements which leads to the simplest expression for the scattered intensity as a function of energy loss E and momentum transfer $\hbar\mathbf{q}$, namely [5,6],

$$I(\mathbf{q}, E) \sim \sum_{\substack{n\mathbf{k} \\ \text{unocc.}}} |\langle n\mathbf{k}|e^{i\mathbf{q}\cdot\mathbf{r}}|c\rangle|^2 \delta(E - \varepsilon_{n\mathbf{k}} + \varepsilon_c)$$

$$\equiv \sum_{\substack{n\mathbf{k} \\ \text{unocc.}}} |M_{\mathbf{q}}|^2 \delta(E - \varepsilon_{n\mathbf{k}} + \varepsilon_c), \tag{2.1}$$

where $\langle \mathbf{r} \mid c\rangle = \varphi_c(\mathbf{r})$ is the core wavefunction from which an electron is ejected, and $\langle \mathbf{r} \mid n\mathbf{k}\rangle = \varphi_{n\mathbf{k}}(\mathbf{r})$ is the conduction band wavefunction, unoccupied in the ground state, to which the electron is excited. Eq. (2.1) has the benefit of a very simple interpretation in the independent electron picture. The squared matrix element is proportional to the rate of transition from one eigenstate to another; the sum is over all possible final states, strictly limited by the delta function which ensures the conservation of energy since it is zero unless $E = \varepsilon_{n\mathbf{k}} - \varepsilon_c$. That is, the energy lost to the beam is the eigenvalue difference between the two levels. We would like to explain the origin of the operator $e^{i\mathbf{q}\cdot\mathbf{r}}$ appearing in the matrix element, and to make clear how the eigenfunctions should be represented in order to account for electron–electron interaction within the one electron framework. We shall also show how one might modify the delta function to account for the finite lifetime of the excited state. Finally we will give practical details of how the scattered intensity can be calculated within the local density approximation to density functional theory.

2.1. Scattering cross-section of an isolated atom—the theory of Bethe

We consider the case of a beam of electrons, arriving one at a time at the foil as dictated by the typically low flux in an electron microscope. The electrons are scattered by atoms in the foil but they arrive and leave in *plane wave states*. We assume that the incident particle velocity is greater than $(Z/137)c$, where Z is the atomic number of the atom and c is the speed of light; restricting us to incident electron energies above $15Z^2$ eV. This assures that the first Born approximation is valid [7], meaning that each electron experiences just one such scattering event and permitting the use of second-order perturbation theory or the *golden rule* of quantum mechanics. The perturbation theory allows us to write the Hamiltonian that describes the scattering as

$$H = H_{\text{atom}} + H_{\text{electron}} + H_{\text{int}}.$$

H_{atom} is the Hamiltonian for an atom in the foil, most generally given (in non-relativistic quantum mechanics) by Eq. (A.8) (Appendix A). H_{electron} is the Hamiltonian of the independent electrons in the beam, and H_{int} is the electrostatic

potential energy of interaction between the fast electron and the nuclear and electronic charges in the atom. If we take it that the atom is stationary at the origin, then (in units of $4\pi\varepsilon_0 = 1$)

$$H_{\text{int}} = -e^2 \left[\frac{Z}{r} - \sum_{j=1}^{Z} \frac{1}{|\mathbf{r} - \mathbf{r}_j|} \right],$$

where $\mathbf{r}$ denotes the position vector of the scattered electron, and $\mathbf{r}_j$ are the positions of the Z electrons in the atom. Neglecting spin coordinates, the Hamiltonian H_{atom} has a complete set of eigenstates, $\psi_n(\mathbf{r}_1, \ldots, \mathbf{r}_Z)$ with eigenvalues E_n, of which the ground state is ψ_0. We should point out that we cannot, even in principle, determine the exact eigenstates of a many body Hamiltonian. However without approximation we can write the eigenstates of $H_{\text{atom}} + H_{\text{electron}}$ as products of a state ψ_n and a plane wave $\mathrm{e}^{\mathrm{i}\mathbf{k}\cdot\mathbf{r}}$. If the incoming electron has wavevector $\mathbf{k}$ and the outgoing electron $\mathbf{k}'$, we define the momentum transfer to the scatterer as $\hbar\mathbf{q} = \hbar(\mathbf{k} - \mathbf{k}')$. To arrive at Bethe's expression for the scattering rate one makes a Fourier transform of H_{int} followed by a discrete back transform [8–10]:

$$H_{\text{int}} = \sum_{\mathbf{q}'} V_{q'} \, \mathrm{e}^{\mathrm{i}\mathbf{q}'\cdot\mathbf{r}} \left(Z - \sum_j \mathrm{e}^{-\mathrm{i}\mathbf{q}'\cdot\mathbf{r}_j} \right),$$

where the Fourier transform of the Coulomb potential is, in unit volume [11],

$$V_q = \frac{4\pi e^2}{q^2}.$$

Because of the low incident flux we may take it that in the initial state the atom is in its ground state and so the initial state of $H_{\text{atom}} + H_{\text{electron}}$ is $|0\rangle = \psi_0 \, \mathrm{e}^{\mathrm{i}\mathbf{k}\cdot\mathbf{r}}$ and the final state, finding the atom in some excited state ψ_n, is $|f_n\rangle = \psi_n \, \mathrm{e}^{\mathrm{i}\mathbf{k}'\cdot\mathbf{r}}$. Then using $\int \mathrm{e}^{\mathrm{i}(\mathbf{q}+\mathbf{q}')\cdot\mathbf{r}} \, \mathrm{d}\mathbf{r} = \delta(\mathbf{q} - \mathbf{q}')$ in unit volume, the matrix element of H_{int} between final and initial states is

$$\langle f_n | H_{\text{int}} | 0 \rangle = -Vq\varepsilon_{0n},$$

where[1]

$$\varepsilon_{mn} = \int \ldots \int \bar{\psi}_n \left(Z - \sum_j \mathrm{e}^{\mathrm{i}\mathbf{q}\cdot\mathbf{r}_j} \right) \psi_m \, \mathrm{d}\mathbf{r}_1 \, \mathrm{d}\mathbf{r}_2 \cdots \mathrm{d}\mathbf{r}_Z.$$

According to the golden rule [7,12] the probability per unit time that the electron is scattered with momentum transfer $\hbar\mathbf{q}$ leaving the atom in the eigenstate ψ_n is $P_{0n}(\mathbf{q}) = (2\pi/\hbar)\rho(\varepsilon)|\langle f_n \mid H_{\text{int}} \mid 0\rangle|^2$.[2] Hence the probability of scattering into any final state, but with an energy loss E, is a sum over all final states, each term multiplied by an energy conserving delta function,

$$P(\mathbf{q}, E) = \frac{2\pi}{\hbar} \rho(\mathcal{E}) \sum_n |\langle f_n | H_{\text{int}} | 0 \rangle|^2 \delta(E - E_n + E_0),$$

where [9,12]

$$\rho(\mathcal{E}) = \frac{v}{(2\pi\hbar)^3} \left(\frac{\mathcal{E}}{c^2} \right)^2 \approx \frac{1}{(2\pi)^3} \frac{mk'}{\hbar^2} \quad (v \ll c)$$

is the density per unit volume of final states of the beam.

If the scattering is inelastic then the *first term* in ε_{mn} vanishes because of orthogonality of the atomic eigenstates. Furthermore the second term is a sum over Z identical integrals because if the coordinate $\mathbf{r}_j$ is exchanged for, say, $\mathbf{r}_1$ in both ψ_n and ψ_m the changes of sign arising from the Pauli principle cancel, hence each term can be written replacing $\mathbf{r}_j$ with $\mathbf{r}_1$. Hence defining the *transition form factor* $F_n(\mathbf{q})$ for excitation of the system to a final state ψ_n as

$$F_n(\mathbf{q}) = Z \int \ldots \int \bar{\psi}_n \, \mathrm{e}^{\mathrm{i}\mathbf{q}\cdot\mathbf{r}_1} \psi_0 \, \mathrm{d}\mathbf{r}_1 \, \mathrm{d}\mathbf{r}_2 \cdots \mathrm{d}\mathbf{r}_Z,$$

and furthermore the *dynamical form factor* [10]

$$S(\mathbf{q}, E) = \sum_n |F_n(\mathbf{q})|^2 \delta(E - E_n + E_0),$$

we finally obtain for the inelastic scattering rate,

$$P(\mathbf{q}, E) = \frac{2\pi}{\hbar} \rho(\mathcal{E}) V_q^2 S(\mathbf{q}, E), \tag{2.2}$$

which is in the form of Eq. (2.1). Note how in the first Born approximation the electron beam acts as a *non-intrusive probe*. The experiment provides a measure of the fluctuations in the unperturbed system, encaptured in the dynamical form factor. Mathematically, this is because the beam electron coordinate has been integrated out [8] in forming the Fourier transform of H_{int}, leaving only the coordinates of the specimen electrons and nuclei (the latter surviving in *elastic* scattering only). The formula (2.2) is essentially exact; it is not clear how to cast this into a one electron form. However the key points are these. (i) The initial and final states ψ_0 and ψ_n are orthogonal eigenfunctions of the same Hamiltonian, H_{atom}. (ii) We will assume that they can be written as single Slater determinants

[1] Bethe [8] defined a *dimensionless generalised transition probability* $\varphi_{mn}(q) = (qa_0)^{-2}|\varepsilon_{mn}(q)|^2$, where $a_0 = \hbar^2/me^2$ is the Bohr radius ($\approx$0.0529 nm) and *generalisierte Oszillatorstärke* (*generalised oscillator strength*) $f_{mn}(q) = \frac{E_n - E_m}{\text{Ry}} \varphi_{mn}(q)$, where Ry is the Rydberg unit of energy $e^2/2a_0$ ($\approx$13.61 eV). He also proved the *f-sum rule*, $\sum_n f_{mn}(q) = Z$ (see also [10, p. 92]).

[2] It follows furthermore from the golden rule that the differential cross-section, with respect to the polar angles of $\mathbf{k}'$, for scattering into final state ψ_n is [9,12] $\sigma(\theta, \phi) = \frac{P_{0n}(\mathbf{q})}{v_0} = \left(\frac{\mathcal{E}}{2\pi\hbar^2 c^2} \right)^2 \frac{v}{v_0} V_q^2 |\varepsilon_{0n}|^2 = \left(1 - \frac{v^2}{c^2} \right) \frac{1}{a_0^2 q^4} \frac{v}{v^0} |\varepsilon_{0n}|^2$, where $\mathcal{E} = \sqrt{1 - v^2/c^2} mc^2$ is the energy of the outgoing electron, including its mass m, and v_0 and v are initial and final electron velocities. This covers both elastic and inelastic scattering. In elastic scattering, $v = v_0$ and $\varepsilon_{0n} = \varepsilon_{00} = (Z - F(\mathbf{q}))$, where $F(\mathbf{q}) = \int \rho(\mathbf{r}) \, \mathrm{e}^{\mathrm{i}\mathbf{q}\cdot\mathbf{r}} \, \mathrm{d}\mathbf{r}$ is the *atomic form factor*. Indeed if one neglects the electronic charge altogether ($F(\mathbf{q}) \to 0$) one recovers the Rutherford formula for scattering by a point charge $|e|Z$ with its characteristic q^{-4} dependence of the cross-section which survives into the inelastic case. Clearly forward scattering into small momentum transfers is greatly favoured.

[11]. By the special properties of Slater determinants, the matrix element of any one electron operator is zero if more than one of the entries is different. Indeed if

$$\psi_m = \frac{1}{\sqrt{N!}} \det|\varphi_k(\mathbf{r}_j)|,$$

and

$$\psi_n = \frac{1}{\sqrt{N!}} \det|\varphi'_k(\mathbf{r}_j)|,$$

then if the operator $f(\mathbf{r}_1)$ is a function only of $\mathbf{r}_1$ and if all the entries φ_i and φ'_i are the same *except one pair*, say, φ_1 and φ'_1 then

$$\int \dots \int \bar{\psi}_n f(\mathbf{r}_1)\psi_m \, \mathrm{d}\mathbf{r}_1 \, \mathrm{d}\mathbf{r}_2 \cdots \mathrm{d}\mathbf{r}_Z$$
$$= \frac{1}{N} \int \bar{\varphi}'_1(\mathbf{r}_1) f(\mathbf{r}_1)\varphi_1(\mathbf{r}_1) \, \mathrm{d}\mathbf{r}_1 \prod_{j=2}^{N} \int \bar{\varphi}'_j(\mathbf{r}_j)\varphi_j(\mathbf{r}_j) \, \mathrm{d}\mathbf{r}_j. \tag{2.3}$$

The matrix element is rigorously a one electron integral, all the overlap integrals following being equal to one. On the other hand if more than one orbital changes then the matrix element vanishes because of orthogonality of the basis functions that make up the Slater determinants, i.e., at least one of the succeeding factors in the product will be zero. It is inconsistent that ψ_n and ψ_m are orthogonal eigenfunctions of a Hamiltonian containing electron–electron interactions while simultaneously being representable as Slater determinants. A further complication arises if while one orbital changes significantly, the others all change by small amounts; an effect that can be produced in a variational calculation, or by demanding that ψ_n and ψ_m are eigenstates of *different* Hamiltonians. For example ψ_n may be an eigenstate of the atomic Hamiltonian including an additional potential due to the core hole. In such cases the one electron matrix element in (2.3) is followed by a product of $N-1$ numbers less than or approximately equal to one and the matrix element may or may not vanish identically as $N \to \infty$. This has been called an orthogonality catastrophe!

2.2. Scattered intensity from an extended crystal—the theory of Hedin

There is an alternative path to (2.1) using the language of many body physics which has a number of instructive features [13]. The question of representation of the initial and final states is more clearly given for an extended system and the matrix element emerges more readily as a one electron integral out of a many body formalism. The Hedin theory lends itself well to the bandstructure approach; possibly the most important benefit is that it provides a clear indication of how the bandstructure calculation can be systematically improved, a point we will address in Section 3.3. In particular we can put into focus the question of how the measured near edge structure relates to the local density of states. We may point out here that in a bandstructure calculation, one calculates the density of states of an N electron system which is in principle not measurable; instead one measures the density of states of an associated $N+1$ electron system (as in X-ray absorption or EELS) or an $N-1$ electron system in the case of photoemission. Hedin's theory was intended to describe soft X-ray emission, we adapt it here for EELS; Appendix A gives some background to the many body problem in Appendix A.1 and describes the "retarded" Green function which is needed in this case in Appendix A.2.

The central assumption of the theory is that the interaction between the valence electrons and the core hole can be fully described as the response of the electron gas to the injection of an additional electron while simultaneously and suddenly a core hole is created. This means that the wavefunctions can be approximated as antisymmetrised products of valence and core wavefunctions. For simplicity here we will write them as Hartree products rather than two by two determinants but the final result is the same. Hence we write the initial state as

$$|i\rangle = |c\rangle|N\rangle$$

the product of the ground state of N valence electrons and the wavefunction of the core electrons in which all core levels are doubly occupied. There is a complete set of states of the $N+1$ valence electron system labelled with an index s and denoted $|N+1, s\rangle$, having total energy ϵ_s (A.9) and the final state is written as a product of this times the core level wavefunction having one core level only singly occupied—a core hole, thus:

$$|f_s\rangle = |c-1\rangle|N+1, s\rangle.$$

Apart from the decoupling of the core and valence wavefunctions no restriction is placed on these otherwise. We shall see that electron–electron interaction is fully taken care of by the spectral density which is the imaginary part of the retarded Green function. Just as in the general Bethe theory where ψ_0 and ψ_n are eigenfunction of the atomic Hamiltonian including electron–electron interaction, so $|N\rangle$ and $|N+1, s\rangle$ are eigenfunctions of the Hamiltonian with interaction (A.8). Now by invoking the golden rule and the representation of $\mathrm{e}^{\mathrm{i}\mathbf{q}\cdot\mathbf{r}}$ in field operators (A.7), we can write

$$P(\mathbf{q}, E) = \frac{2\pi}{\hbar}\rho(\mathcal{E})V_q^2 \sum_s \left| \langle f_s | \int \psi^\dagger(\mathbf{r}) \, \mathrm{e}^{\mathrm{i}\mathbf{q}\cdot\mathbf{r}} \psi(\mathbf{r}) \, \mathrm{d}\mathbf{r} | i \rangle \right|^2 \times \delta(E - \epsilon_s + \epsilon_c)$$
$$\equiv \frac{2\pi}{\hbar}\rho(\mathcal{E})V_q^2 \sum_s |M_s|^2 \delta(E - \epsilon_s + \epsilon_c), \tag{2.5}$$

where ϵ_c is the total energy of the ground state with the core level occupied. Note that a quantity like ϵ_s is not a one electron eigenvalue; rather a pole of the one electron Green function (A.11). Now we write the field operators, without

approximation as (cf. (A.4))

$$\psi(\mathbf{r}) = \psi_c(\mathbf{r}) + \psi_v(\mathbf{r}) = \sum_c a_c\varphi_c(\mathbf{r}) + \sum_{n\mathbf{k}} a_{n\mathbf{k}}\varphi_{n\mathbf{k}}(\mathbf{r}), \tag{2.6}$$

where a_c and $a_{n\mathbf{k}}$ are annihilation operators for one electron core and valence states, respectively. When (2.6) is inserted into (2.5) we observe that the second term in $\psi(\mathbf{r})$ acting to the right produces an N particle state that will give zero when integrated with the $N+1$ particle state on the left; similarly the first term in $\Psi^\dagger(\mathbf{r})$ acting to the left produces a vector $\langle c-2|$ which will produce zero when integrated with the state on the right. Hence, since $\psi_c(\mathbf{r})$ only acts on core functions and $\psi_v(\mathbf{r})$ only on valence functions, the matrix element in (2.5) becomes

$$M_s = \int \langle N+1, s|\psi_v^\dagger(\mathbf{r})|N\rangle\langle c-1|\psi_c(\mathbf{r})|c\rangle\, \mathrm{e}^{\mathrm{i}\mathbf{q}\cdot\mathbf{r}}\,\mathrm{d}\mathbf{r}.$$

Note that by neglecting dynamical interaction between the core hole and the excited electron, the transition rate becomes the product of two independent rates: the rate of core hole production and the rate of valence excitation. Now $\langle c-1|\psi_c(\mathbf{r})|c\rangle$ is non-zero only when the core level in expansion (2.6) is the particular core level to be excited (for which we will retain the label c), so it becomes simply $\varphi_c(\mathbf{r})$ and expanding $\psi_v^\dagger(\mathbf{r})$ we obtain

$$\begin{aligned} M_s &= \int \varphi_c(\mathbf{r})\langle N+1, s\left|\sum_{n\mathbf{k}} a_{n\mathbf{k}}^\dagger\bar{\varphi}_{n\mathbf{k}}(\mathbf{r})\right| N\rangle\, \mathrm{e}^{\mathrm{i}\mathbf{q}\cdot\mathbf{r}}\,\mathrm{d}\mathbf{r} \\ &= \sum_{n\mathbf{k}} \int \varphi_c(\mathbf{r})\,\mathrm{e}^{\mathrm{i}\mathbf{q}\cdot\mathbf{r}}\bar{\varphi}_{n\mathbf{k}}(\mathbf{r})\,\mathrm{d}\mathbf{r}\langle N+1, s|a_{n\mathbf{k}}^\dagger|N\rangle \\ &= \sum_{n\mathbf{k}} M_{\mathbf{q}}\langle N+1, s|a_{n\mathbf{k}}^\dagger|N\rangle, \end{aligned}$$

where $M_{\mathbf{q}}$ is exactly the matrix element in (2.1). Comparing now with the diagonal spectral density (A.12) and neglecting off-diagonal terms [13], we finally find from (2.5)

$$\begin{aligned} P(\mathbf{q}, E) &= \frac{2\pi}{\hbar}\rho(\mathcal{E})V_q^2\sum_s\left|\sum_{n\mathbf{k}} M_{\mathbf{q}}\langle N+1, s|a_{n\mathbf{k}}^\dagger|N\rangle\right|^2 \\ &\quad\times\delta(E-\epsilon_s+\epsilon_c) \\ &= \frac{2\pi}{\hbar}\rho(\mathcal{E})V_q^2\sum_{n\mathbf{k}}|M_{\mathbf{q}}|^2 A_{n\mathbf{k}}(E+\epsilon_c). \end{aligned}$$

This expression encompasses all the electronic relaxation due to the creation of the core hole and the injection of an additional electron into the conduction bands, all electron–electron interactions being taken care of by the spectral density which is the imaginary part of the one electron Green function and *which multiplies a matrix element involving only single particle states*. Calculation of the spectral density is possible within the GW approximation of Hedin and Lundqvist [14] (Appendix A.3), whereas in the usual density functional approach one uses (A.13) to obtain finally

$$I(\mathbf{q}, E)\sum_{n\mathbf{k}}|M_{\mathbf{q}}|^2\delta(E+\varepsilon_c-\varepsilon_{n\mathbf{k}}),$$

which is (2.1) where ε_c and $\varepsilon_{n\mathbf{k}}$ are now single particle eigenvalues of the core and valence levels, respectively.

3. Results of calculations

This section presents calculations based upon the theory presented, and comparisons with experiment. The calculations use the all-electron LMTO scheme [15] which is outlined in Appendix B along with details about the calculation of the transition matrix elements. Apart from treating core and valence electrons self-consistently, the principal advantage of the LMTO method is its efficiency without sacrificing accuracy in the search for the exact solution to the local density equations. This permits the relaxation of a 100 or more atoms without trouble using molecular statistics as well as the calculation of properties such as the near edge structure in EELS. It was emphasised elsewhere that for reliable predictions, one requires a method giving accurate *atomic* as well as *electronic* structures [16].

We need to summarise a few points about the representation of the wavefunctions that are used to construct matrix elements. It is clear from Bethe's theory that the golden rule requires us to take matrix elements of the interaction H_{int} between orthogonal eigenstates of the atomic Hamiltonian H_{atom}. Due to the orthogonality the interaction appears as the operator $\mathrm{e}^{\mathrm{i}\mathbf{q}\cdot\mathbf{r}}$; and again due to orthogonality the expansion of this (B.6) allows us to reject the first term. We have also seen that the question of orthogonality in practice is troublesome, since we cannot construct exact eigenstates of the many electron Hamiltonian (A.8). LMTO valence states such as (B.5) are orthogonal to each other and to the core states as long as they are eigenstates of the same Kohn–Sham equations (B.2); if we calculated valence and core states in a different potential, say with a core hole potential, the valence and core states are not orthogonal to those constructed in the ground state potential. This is because the LMTO's are not a fixed basis set, but depend on the potential. We should note that to the core hole potential is also added the Hartree and exchange correlation potentials due to the additional electron in the conduction band. The solid state theory of Hedin makes it clear that even if we are working with eigenfunctions of the Hamiltonian (A.8), the transition rate is given by a squared matrix element between one electron eigenstates of a non-interacting Hamiltonian (A.2) multiplied by a spectral density that takes care of electron–electron interactions. In a mean field, or independent electron picture such as density functional theory in the local density approximation, we can take this to be merely a delta function. So while it is neither convenient, nor necessary, to use different Hamiltonians for the final and initial states, what about the core hole potential? Should this be included in the Hamiltonian? The

answer is yes, in the sudden approximation. The Hedin picture is quite clear: the fast particle instantly creates a core hole, switching on a potential additional to that seen by the valence and core electrons in the ground state. Simultaneously the core electron is injected into the valence system, therefore its propagator, or Green function, is the one associated with a Hamiltonian including an additional one electron potential due to the core hole. Happily in the local density and GW approximations, we can construct one electron orthogonal eigenstates and hence matrix elements, as outlined in Appendix B. One may think of the electronic structure as a self-consistent ground state under the constraint that a certain core occupancy is 1, not 2.

3.1. Chromium nitride

The rather complex antiferromagnetic structure of CrN has been described as distorted rocksalt [17,18], and energy comparisons between competing magnetic and non-magnetic phases using the local spin density approximation [6,19] agree with the experimental finding that CrN occurs in a structure with space group *Pnma* having Cr and N atoms in 4(*c*) Wyckoff positions: $x, \frac{1}{4}, z$; $-x, \frac{3}{4}, -z$; $\frac{1}{2}-x, \frac{3}{4}, \frac{1}{2}+z$; $\frac{1}{2}+x, \frac{1}{4}, \frac{1}{2}-z$ with $x \sim \frac{1}{8}, z \sim \frac{1}{4}$ for Cr, and $x \sim \frac{1}{8}$, $z \sim \frac{3}{4}$ for *N*. There are eight atoms in the primitive unit cell. Minimising the energy with respect to lattice parameters and internal coordinates we find $x = 0.146$, $z = 0.250$ for Cr, $x = 0.099$, $z = 0.750$ for *N*; $a = 5.645$ Å, $b = 2.988$ Å, $c = 4.105$ Å. LMTO calculations were done using a double set of s, p and d basis functions augmented in atomic spheres of radius 2.6 bohr (Cr) and 1.8 bohr (N). The large, and slightly overlapping, sphere radii obviate the need to include semicore Cr 3p functions in the basis set. Smoothing radii were half the atomic sphere radii and Hankel function localisation energies in the two sets were −0.01 and −0.1 Ry.

Fig. 1 shows nitrogen near *K*-edge structure calculated with one nitrogen core hole in the primitive unit cell; and also in a unit cell (or *supercell*) with dimensions doubled in all three directions (i.e., containing 64 atoms) and containing just one core hole on a nitrogen atom. In these calculations we have averaged over the scattering vector, **q**, as explained in previous work [6]. We also show the *absolutely predicted* energy loss. The threshold energy was determined using the Slater transition state approximation and reduced by 4.22 eV which was found previously to be applicable universally to the transition metal carbides and nitrides [6]. The point here is that we wish to make the best attempt at calculating the threshold energy, something which is not usually done in the literature (instead the spectra are aligned on the energy axis by eye). In the case of the transition metal nitrides and carbides we found that whereas the threshold energies calculated for independent electrons was in error by some 20 eV and very scattered, when calculated using the Slater transition state approximation the error was a rather uniform 4.22 eV. If we apply this shift we then get an ab initio prediction of the absorption edge and further adjustment when comparing to experiment is not permitted. This is how Fig. 1 is constructed.

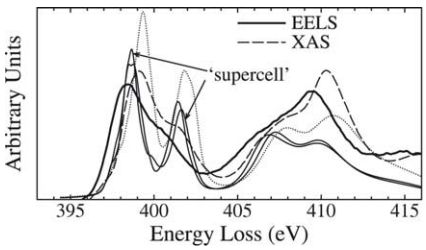

Fig. 1. Calculated and measured nitrogen *K*-edge energy loss spectra in antiferromagnetic, orthorhombic CrN. The experimental EELS and X-ray absorption data are from Paxton et al. [6]; the estimated error in the absolute energy loss is ±0.5 eV. The theoretical threshold is obtained using the Slater transition state approximation and a downward shift of 4.22 eV which was found to apply universally in transition metal carbides and nitrides [6]. The thin solid lines are the calculated spectra with the inclusion of a core hole and the use of primitive (8 atoms) and 2 × 2 × 2 (64 atoms) unit cells. The dotted line is the calculation in the absence of the core hole.

Also in Fig. 1 is shown the spectrum obtained from a calculation without a core hole. Compared to the experimental EELS spectrum we see that peak positions are in better agreement from the "final state" basis. Fig. 1 also shows the X-ray absorption spectrum which includes the second peak as a shoulder rather more strongly than the EELS spectrum. We have applied a Lorentzian broadening only, using (A.14) with the plasmon energy calculated from the average electron density, to which is added 0.2 eV to account for the lifetime of the core level. We do not apply instrumental broadening in order to illustrate *theoretical* peak shapes. We attribute the reduction of the second peak to a shoulder in the experiment to magnetic disordering although the spectrum remains the same even at temperatures well below the Neel temperature [6]. Furthermore it has recently been argued that one cannot distinguish short and long ranged magnetic ordering in an EELS experiment because of the small region of crystal and the short period of time over which the interaction happens between the beam and specimen [20]. There is need for further work to elucidate this point.

Fig. 2 shows the difference in valence electron density between the self-consistent ground states with and without the core hole, calculated using the 64-atom supercell. The positive contours show where the charge accumulates to screen the core hole. The spin density difference shows that the total moment changes from zero in the antiferromagnetic ground state to about $0.1\mu_B$: the excited electron is spin polarised. Note that the screening charge is fairly well localised to between the first and second neighbour shell of the nitrogen atom. The spin density is very well localised to within the atomic sphere radius of the nitrogen atom, that is to say the majority of the spin moment is localised at the excited nitrogen atom.

3.2. Monoclinic zirconia

The second example is monoclinic zirconia which is chosen because this is the phase that can be prepared in a pure

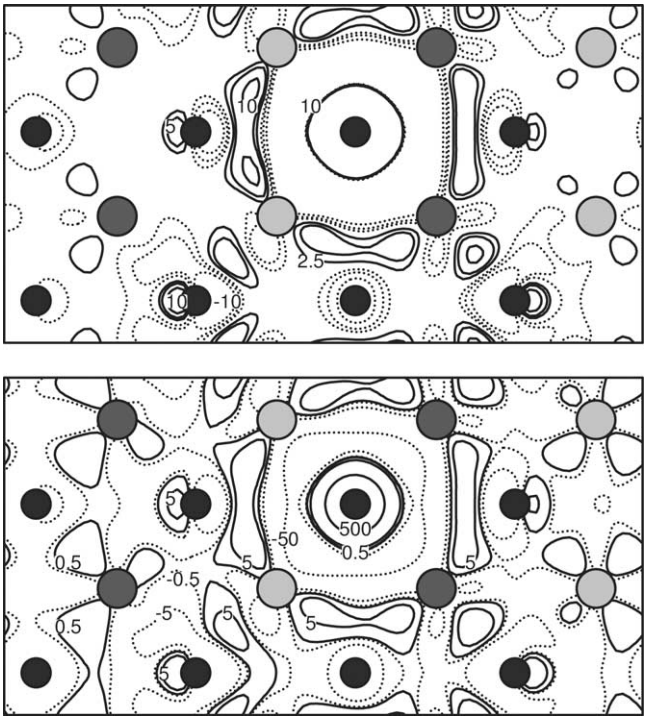

Fig. 2. A section through the *a*–*b* plane of orthorhombic CrN cutting through the nitrogen at which there is a core hole. The reader can see the face of the distorted rocksalt structure rotated by 45°: large, dark circles are Cr atoms with spin "up", large light circles are Cr atoms with spin "down", smaller circles are N atoms. The contours are electron density differences between the ground states with and without the hole and hence show the rearrangement of charge created by the core excitation. The upper panel shows the density difference and the lower panel the spin density difference, up minus down. Contours are ±10, ±5 and ±2.5 in the upper panel and ±500, ±50, ±5 and ±0.5 in the lower panel with dotted lines denoting negative values. Units are 10^{-4} electrons bohr^{-3}.

crystal. LMTO calculations were done using, on the zirconium atoms, one set of s, p, d and f functions with localisation energies −0.01 Ry and a second set of s, p and d only with localisation energies −5, −2 and −2 Ry, augmented in atomic spheres of radius 2.3 bohr. In addition local orbitals [21] were used to represent the 4s and 4p semicore states. On the oxygen atoms, the basis functions were s, p and d with localisation energies −0.01 and −1 Ry, the oxygen atomic sphere radius was 1.8 bohr. The monoclinic crystal has space group $P2_1/c$ and the lattice parameters and internal coordinates were determined by energy minimisation to be $a = 5.071$ Å, $b = 5.191$ Å, $c = 5.278$ Å, $\beta = 99.17°$; $x_{Zr} = 0.281$, $y_{Zr} = 0.041$, $z_{Zr} = 0.211$, $x_{O(I)} = 0.070$, $y_{O(I)} = 0.335$, $z_{O(I)} = 0.344$, $x_{O(II)} = 0.448$, $y_{O(II)} = 0.758$, $z_{O(II)} = 0.480$. These are an improvement compared to experiment and other LDA calculations on those reported earlier [22] due to the inclusion of local orbitals in the present work.

Fig. 3 shows calculated EELS spectra in the primitive 12-atom unit cell and in a supercell of 96 atoms. In this case, since the crystal is an insulator and therefore screening of the core hole is less efficient than in a metal, there is some shift of the first peak in the supercell to coincide rather better

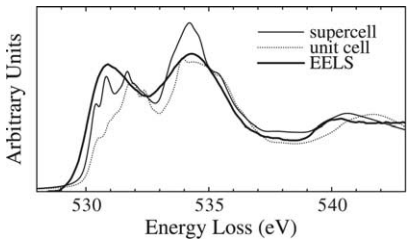

Fig. 3. Calculated and measured oxygen *K*-edge energy loss spectra in monoclinic ZrO_2. The experimental EELS spectrum is taken from Ostanin et al. [24]; the uncertainty in the absolute energy loss is ±1 eV. The theoretical curves have been shifted down by 6 eV to line up the spectra. The $2 \times 2 \times 2$ supercell shows significantly improved agreement with the experiment.

with the experiment. A similar effect has been found in MgO using the "$Z + 1$" approximation to model the core hole [25]. The threshold energy predicted by the Slater transition state approximation is 535.763 eV on oxygen(I) and 536.467 eV on oxygen(II). The calculated spectrum is the sum of these shifted with respect to each other to account for the chemical shift of 0.704 eV. Finally the summed spectra are shifted by a further 6 eV to bring the peak into coincidence with the experiment. This 6 eV is the error from the local density approximation in the transition state. The spectra were broadened using (A.14), with a plasmon energy of 26 eV obtained experimentally [23].

Fig. 4 shows, as in Fig. 2, the electron density associated with the core hole. The perturbation is more long ranged than in metallic CrN and can be seen to have the effect of polarising the charge on the neighbouring zirconium as well as oxygen ions. This longer range is consistent with the difference in spectra between the primitive unit cell and the supercell. It may seem puzzling that the charge differences are mostly associated with the neighbouring Zr ions, and that these are dipole polarised contrary to the notion that it is the anions that are most polarisable. However the unoccupied states at the conduction band edge are largely Zr-derived in an ionic picture, hence the weight is largely on the cation. Furthermore these are d-states: the dipoles observed are caused by the electrostatic effect of the nearby core hole potential. This reinforces the point that in oxides, and ionic crystals in general, the *anion K*-edges reveal the electronic structure of the *cation*-derived energy bands.

3.3. Nickel oxide

A final example is cubic NiO whose electronic structure has been the subject of vivid controversy over the last 20 years. The local spin density approximation (LSDA) correctly predicts NiO to be an antiferromagnetic insulator with the (1 1 1) magnetic ordering found in MnO [26]. However LSDA also predicts a band gap of only 0.3 eV; indeed the crystal is predicted to be metallic under other magnetic orderings [26]. On the other hand highly correlated configuration interaction schemes predict a band gap of about 4 eV, consistent with experiment [27]. It is now accepted that NiO is neither a

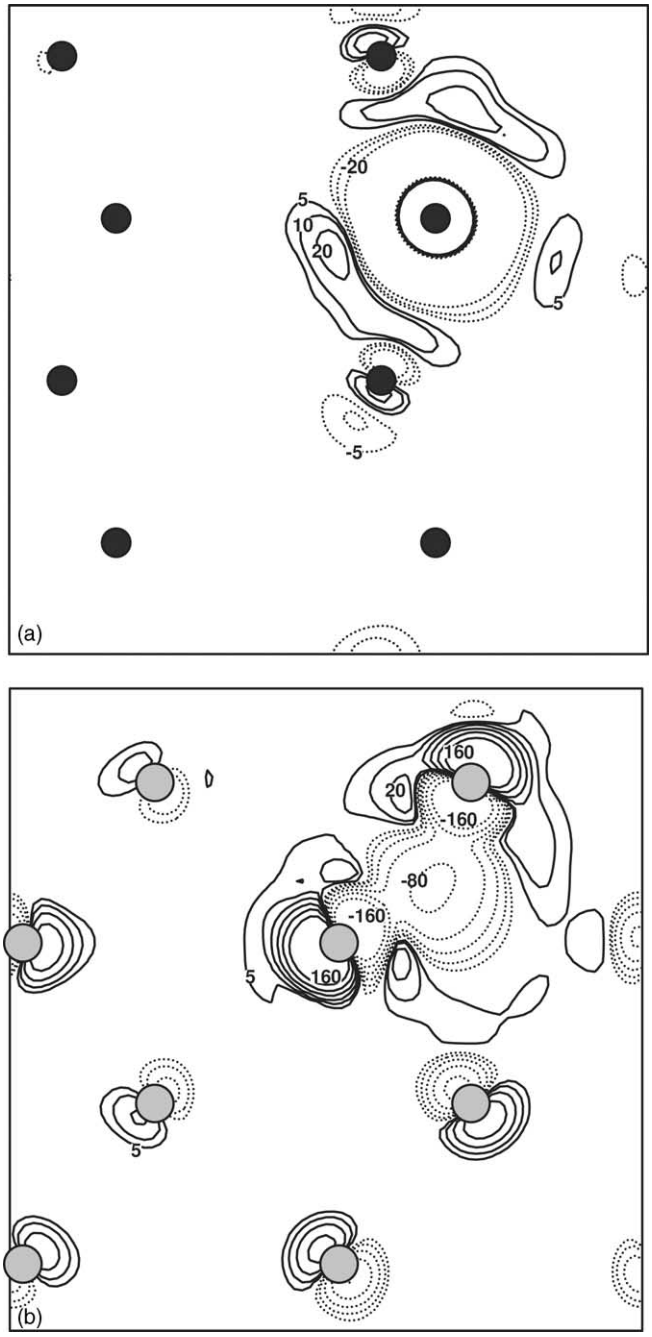

Fig. 4. Sections through the *b*–*c* plane of monoclinic ZrO_2 showing electron density differences between the ground states with and without a core hole. Contours are ±20, ±10 and ±5 in units of 10^{-4} electrons bohr^{-3} with dotted lines denoting negative values. The sections cut through (a) the oxygen with a core hole (this is an O(I) atom which is three-fold coordinated to Zr); and (b) a Zr to which the O(I) is bonded in the neighbouring plane.

Mott–Hubbard nor a charge transfer insulator, but something in between [28]. Whether the electronic structure can be represented in a one electron picture is still under debate, as is the nature of the occupied and unoccupied electronic states. Recently schemes developed for handling electron correlation better than LDA, such as LDA + *U* [29] and the GW approximation [30], have been used to calculate the electronic structure of NiO, but the band gap is still not correctly rendered in these schemes. However, very recently Faleev et al. [31], have developed a *self-consistent* GW approximation implemented using the LMTO basis which correctly reproduces the band gap and electronic structure of NiO. Rather surprisingly they conclude that the LSDA makes a better starting point than the configuration interaction picture for the description of the unoccupied bands. In Fig. 5 we show the oxygen near *K*-edge structure in both LSDA and the self-consistent GW approximation, compared with experimental data taken from Dudarev et al. [29], who compared their data with LDA + *U* calculations. In the latter scheme the Coulomb integral *U* has to be assigned semi-empirically, whereas the GW approximation, like LSDA is parameter free. These preliminary calculations have been made using the GW quasiparticle energies obtained by replacing V_{xc} in the one electron Kohn–Sham equations by the self-energy Σ [16]. However the spectral function was not computed: instead a Gaussian broadening was used. Furthermore spectra were calculated without a core hole from which we would expect downward shifts of about 1 eV. Even this simplified GW approximation demonstrates a significant improvement over the LSDA. However the agreement is not as good as expected from, say, the results in Fig. 3. It will be very interesting to extend the calculation by including the explicitly calculated spectral density [30]. Clearly the GW approximation is the most natural way to go beyond the LDA, therefore these first calculations are a very exciting indication of the future for the prediction of near edge structure in electron energy loss spectroscopy.

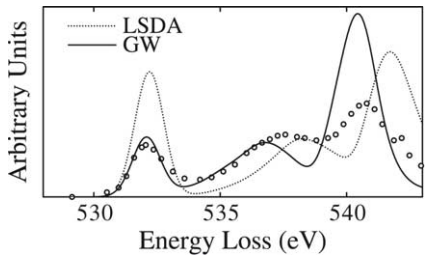

Fig. 5. Calculated and measured oxygen *K*-edge energy loss spectra in NiO. Experimental points are from Dudarev et al. [29]. Dotted and solid lines are taken from calculations by Faleev et al. [31] using the local spin density and GW approximations (see the text for details). The spectra have been aligned so that the first peaks coincide.

Acknowledgements

I should like to thank Alan Craven for provoking my interest in this topic and for countless invaluable conversations. Mark van Schilfgaarde very kindly allowed access to his unpublished material. I have benefited greatly from discussions with Tchavdar Todorov.

Appendix A. Short introduction to many body theory

A.1. The Schrödinger equation

Following Haken [32], let us think of the Schrödinger equation for a single particle and its Hermitian conjugate as classical wave equations:

$$-\frac{\hbar^2}{2m}\nabla^2\psi + V(\mathbf{r})\psi = \mathrm{i}\hbar\dot{\psi}, \tag{A.1}$$

$$-\frac{\hbar^2}{2m}\nabla^2\psi^* + V(\mathbf{r})\psi^* = -\mathrm{i}\hbar\dot{\psi}^*$$

in terms of independent variables ψ and ψ^* (or equivalently the real and imaginary parts of ψ). If we construct a Lagrangian

$$L = \int \psi^* \left(\mathrm{i}\hbar\dot{\psi} - V(\mathbf{r})\psi + \frac{\hbar^2}{2m}\nabla^2\psi\right) \mathrm{d}\mathbf{r},$$

then the Lagrangian equation of motion leads directly to the Schrödinger equation:

$$\frac{\mathrm{d}}{\mathrm{d}t}\frac{\delta L}{\delta\dot{\psi}^*} - \frac{\delta L}{\delta\psi^*} = -\left(\mathrm{i}\hbar\dot{\psi} - V(\mathbf{r})\psi + \frac{\hbar}{2m}\nabla^2\psi\right) = 0.$$

We therefore form the canonically conjugate momentum

$$\pi = \frac{\delta L}{\delta\dot{\psi}} = \mathrm{i}\hbar\psi^*$$

in order to form the Hamiltonian

$$H = \int \pi\dot{\psi}\,\mathrm{d}\mathbf{r} - L$$

$$= \int \left(\mathrm{i}\hbar\dot{\psi}\psi^* - \mathrm{i}\hbar\psi^*\dot{\psi} - \psi^*\frac{\hbar^2}{2m}\nabla^2\psi + \psi^* V(\mathbf{r})\psi\right) \mathrm{d}\mathbf{r}.$$

Since the first two terms in parentheses cancel we find the Hamiltonian is

$$H = \int \psi^*(\mathbf{r})\left(-\frac{\hbar^2}{2m}\nabla^2 + V(\mathbf{r})\right)\psi(r)\,\mathrm{d}\mathbf{r}. \tag{A.2}$$

One may regard (A.2) as a *fundamental postulate* of quantum mechanics accompanied by the following commutation relations which serve to quantise this Hamiltonian by transforming the "classical" quantities $\psi(\mathbf{r})$ and $\psi^*(\mathbf{r})$ into *field operators* $\psi(\mathbf{r})$ and $\psi^\dagger(\mathbf{r})$ for which

$$[\psi(\mathbf{r}'), \psi^\dagger(\mathbf{r})] = \psi(\mathbf{r}')\psi^\dagger(\mathbf{r}) - \psi^\dagger(\mathbf{r})\psi(\mathbf{r}') = \delta(\mathbf{r}-\mathbf{r}'),$$

$$[\psi(\mathbf{r}), \psi(\mathbf{r}')] = \psi(\mathbf{r})\psi(\mathbf{r}') - \psi(\mathbf{r}')\psi(\mathbf{r}) = 0,$$

$$[\psi^\dagger(\mathbf{r}), \psi^\dagger(\mathbf{r}')] = \psi^\dagger(\mathbf{r})\psi^\dagger(\mathbf{r}') - \psi^\dagger(\mathbf{r}')\psi^\dagger(\mathbf{r}) = 0$$

for bosons, and

$$[\psi(\mathbf{r}'), \psi^\dagger(\mathbf{r})]_+ = \psi(\mathbf{r}')\psi^\dagger(\mathbf{r}) + \psi^\dagger(\mathbf{r})\psi(\mathbf{r}') = \delta(\mathbf{r}-\mathbf{r}'),$$

$$[\psi(\mathbf{r}), \psi(\mathbf{r}')]_+ = \psi(\mathbf{r})\psi(\mathbf{r}') + \psi(\mathbf{r}')\psi(\mathbf{r}) = 0,$$

$$[\psi^\dagger(\mathbf{r}), \psi^\dagger(\mathbf{r}')]_+ = \psi^\dagger(\mathbf{r})\psi^\dagger(\mathbf{r}') + \psi^\dagger(\mathbf{r}')\psi^\dagger(\mathbf{r}) = 0$$

for fermions. This fermion commutator was first shown by Jordan and Wigner to be equivalent to the Pauli principle, basically because the number operators always turn out to be 0 or 1.

It is useful to remember that the "classical" Schrödinger equation (A.1) contains a Hamiltonian operator $-\nabla^2 + V$ and the Hamiltonian in second quantisation

$$H = \int \psi^\dagger(\mathbf{r})\left(-\frac{\hbar^2}{2m}\nabla^2 + V(\mathbf{r})\right)\psi(\mathbf{r})\,\mathrm{d}\mathbf{r} \tag{A.3}$$

is also an operator *but these are not the same thing*. In the first case, the Hamiltonian acts upon an eigenfunction, say $\varphi_i(\mathbf{r})$, which is a function of position, yielding its eigenvalue E_i; the second quantised Hamiltonian (A.3) acts upon a (possibly many body) eigenfunction Φ in an abstract way through the influence of position-dependent field operators. So the second quantised Schrödinger equation is $H\Phi = E\Phi$ and E is the expectation value of the total energy.

Fundamental to many body physics is the expansion of the field operators in terms of single-particle solutions of the time-independent Schrödinger equation

$$-\frac{\hbar^2}{2m}\nabla^2\varphi_i(\mathbf{r}) + V(\mathbf{r})\varphi_i(\mathbf{r}) = E_i\varphi_i(\mathbf{r}).$$

This is because the one-particle problem is usually thought of as soluble so the $\varphi_i(\mathbf{r})$ are known and

$$\psi(\mathbf{r}) = \sum_i a_i\varphi_i(\mathbf{r}), \tag{A.4a}$$

$$\psi^\dagger(\mathbf{r}) = \sum_i a_i^\dagger\bar{\varphi}_i(\mathbf{r}) \tag{A.4b}$$

defines creation and annihilation operators for single-particle states which obey the commutation relations

$$[a_i, a_j^\dagger] = \delta_{ij}, \qquad [a_i, a_j] = 0, \qquad [a_i^\dagger, a_j^\dagger] = 0$$

with equivalent anticommutation relations for fermions:

$$[a_i, a_j^\dagger]_+ = \delta_{ij}, \qquad [a_i, a_j]_+ = 0, \qquad [a_i^\dagger, a_j^\dagger]_+ = 0. \tag{A.5}$$

The ground state Φ_0 is called the *vacuum state* in many-body physics and is defined as

$$a_i\Phi_0 = 0 \quad \text{for all } i,$$

and the solutions of the Schrödinger equation, if H is given by (A.3), are constructed from the vacuum state as

$$\Phi = \prod_i (a_i^\dagger)^{n_i}\Phi_0,$$

where n_i are the occupation numbers of state i, which for fermions are either 0 or 1. Because of the commutation relations the Pauli principle is built in to this wavefunction which is hence exactly equivalent to a single Slater determinant.

It is instructive to work through a few examples. The *particle density operator* in second quantisation is

$$\rho(\mathbf{r}) = \psi^\dagger(\mathbf{r})\psi(\mathbf{r}),$$

and we can construct its expectation value as the bracket

$$\langle \Phi|\psi^\dagger(\mathbf{r})\psi(\mathbf{r})|\Phi\rangle.$$

If Φ is the single particle eigenfunction

$$\Phi = a_k^\dagger \Phi_0, \tag{A.6}$$

then the expectation value of the particle density operator is

$$\left\langle a_k^\dagger \Phi_0 \left| \sum_i a_i^\dagger \phi_i^* \sum_j a_j \phi_j \right| a_k^\dagger \Phi_0 \right\rangle.$$

The trick is to get all the annihilation operators over to the right where they produce zero when they operate on the vacuum state. Freely using the commutation relations (A.5) it is found that the expectation value for this eigenfunction is simply $\phi_k^*(\mathbf{r})\phi_k(\mathbf{r})$ which is what is expected since this is just the single particle density matrix element.

Another example is the position operator in second quantisation,

$$\int \psi^\dagger(\mathbf{r}) x \psi(\mathbf{r})\,\mathrm{d}\mathbf{r}. \tag{A.7}$$

Using again the eigenfunction (A.6) we soon get for the expectation value of the position operator

$$\int \phi_k^*(\mathbf{r}) x \varphi_k(\mathbf{r})\,\mathrm{d}\mathbf{r}$$

as expected. It is more interesting to work out the expectation value of the position operator in the two particle eigenfunction

$$\Phi = a_k^\dagger a_l^\dagger \Phi_0.$$

One finds

$$\int \phi_k^*(\mathbf{r}) x \phi_k(\mathbf{r})\,\mathrm{d}r + \int \phi_l^*(\mathbf{r}) x \phi_l(\mathbf{r})\,\mathrm{d}\mathbf{r}.$$

A.2. The one electron Green function

Let us concentrate specifically on electrons, and in particular on the problem encountered in electron energy loss spectroscopy when an additional electron is excited from a core level, and "injected," into the conduction band of the crystal. In many body theory such a process is described by the one electron Green function associated with the Hamiltonian

$$H = \int \psi^\dagger(\boldsymbol{r}) \left(-\frac{\hbar^2}{2m}\nabla^2 + V(\mathbf{r}) \right) \psi(\mathbf{r})\,\mathrm{d}\mathbf{r} + \frac{1}{2}\int \psi^\dagger(\mathbf{r})\psi^\dagger(\boldsymbol{r}')W(\boldsymbol{r}\boldsymbol{r}')\psi(\boldsymbol{r}')\psi(\mathbf{r})\,\mathrm{d}\mathbf{r}\,\mathrm{d}\boldsymbol{r}', \tag{A.8}$$

where the final term accounts for electron–electron interaction and

$$W(\mathbf{r}\mathbf{r}') \equiv \frac{e^2}{|\mathbf{r}-\mathbf{r}'|}.$$

The Green function is [14]

$$G(\mathbf{r}t, \mathbf{r}'t') = -\mathrm{i}\langle N|\psi(\mathbf{r}, t)\psi^\dagger(\mathbf{r}', t')|N\rangle,$$

which is intended to describe all possible events in which a particle is created in the ground state of N electrons, $|N\rangle$, at time t' and destroyed at a later time t. It is the *probability amplitude* that an electron created at $\mathbf{r}'$ at time t' will be found at $\mathbf{r}$ at a later time t. Hence in principle the Green function contains all the information needed to describe the EELS spectrum. Here $\psi(\mathbf{r}, t)$ is the annihilation field operator in the Heisenberg representation,

$$\psi(\mathbf{r}, t) = \mathrm{e}^{\mathrm{i}Ht/\hbar}\psi(\mathbf{r})\,\mathrm{e}^{-\mathrm{i}Ht/\hbar}.$$

In order to account for all possible excited states of the injected electron, one inserts a complete set of eigenstates of H having $N+1$ electrons. These are denoted $|N+1, s\rangle$ in which s labels the particular excited state. Then if the total energy of the ground state is E_N and of the sth excited state is $E_{N+1,s}$ we may define

$$\epsilon_s = E_{N+1,s} - E_N, \tag{A.9}$$

and

$$f_s(\mathbf{r}) = \langle N|\psi(\mathbf{r})|N+1, s\rangle. \tag{A.10}$$

The Green function is Fourier transformed from time to energy variable [14] and becomes

$$G(\mathbf{r}\mathbf{r}', \epsilon) = \sum_s \frac{f_s(\mathbf{r})\bar{f}_s(\mathbf{r}')}{\epsilon - \epsilon_s - i0}, \tag{A.11}$$

where "0" denotes a positive infinitesimal number. Note that the poles of the Green function are the excitation energies of the system. Using the "Dirac" identity,[3] the imaginary part of $G(\mathbf{r}\mathbf{r}', \epsilon)$ is π times the *spectral function*,

$$A(\mathbf{r}\mathbf{r}', \epsilon) = \sum_s f_s(\mathbf{r})\bar{f}_s(\mathbf{r}')\delta(\epsilon - \epsilon_s),$$

and it is this quantity that is of most interest for us, particularly when represented in the basis of single particle states used to expand the field operators in (A.4). This is called the spectral weight function and is written

$$A_{ij}(\epsilon) = \iint \bar{\varphi}_i(\mathbf{r}) A(\mathbf{r}\mathbf{r}', \epsilon)\varphi_j(\mathbf{r}')\,\mathrm{d}\mathbf{r}\,\mathrm{d}\mathbf{r}',$$

and if we insert the expansion (A.4) into (A.10), we find for a diagonal element,

$$A_j(\epsilon) = \sum_s |\langle N+1, s|a_j^\dagger|N\rangle|^2 \delta(\epsilon - \epsilon_s). \tag{A.12}$$

[3] $\lim_{y\to 0^+} \frac{1}{x \pm \mathrm{i}y} = P\frac{1}{x} \mp \mathrm{i}\pi\delta(x)$ (P denotes "principal value").

Hedin and Lundqvist [14] work out a number of examples for model systems. If the electrons are independent, that is, non-interacting then the spectral weight function becomes simply

$$A_k(\epsilon) = \delta(\epsilon - \varepsilon_k), \tag{A.13}$$

where ε_k is the eigenvalue of the one electron state k. If the electrons are in "decaying states," which is an approximation to the situation experienced by an excited electron in the unoccupied part of the energy bands of a solid then

$$A_k(\epsilon) = \frac{1}{\pi}\frac{\Gamma}{(\epsilon - \varepsilon_k)^2 + \Gamma^2}.$$

This function describes a Lorentzian lineshape in which $\hbar/\Gamma$ is the lifetime of the electron that has been excited by the incoming electron beam. In an independent electron model, such as that described by conventional band theory (see Appendix B) electrons have infinite lifetimes. Interactions serve to limit the time an electron may remain in an excited state since it will lose energy by, for example, Auger processes. In the case of an interacting free electron gas (so-called "jellium") it has been shown that the lifetime is given by [10]

$$\Gamma = \frac{\pi^2\sqrt{3}}{128}E_{\mathrm{p}}\left(\frac{\varepsilon_k - E_{\mathrm{F}}}{W}\right)^2 \tag{A.14}$$

in which E_{F} is the Fermi energy, E_{p} is the plasmon energy and W is the width of the occupied part of the band. The plasmon energy may taken from the low loss region of the EELS spectrum, or calculated from the formula $E_{\mathrm{p}} = 4\sqrt{\pi n}$ Ry, where n is the number of valence electrons per unit volume.

A.3. The GW approximation

The density functional theory is described in Appendix B. This theory which has very wide ranging consequences in physics and materials science is based on the transformation of the many body problem into a set of single particle Schrödinger equations, each particle moving in the *effective potential* $V_{\mathrm{eff}}(\mathbf{r}) = V_{es}(\mathbf{r}) + V_{xc}(\mathbf{r})$ of the other particles. This makes this a *mean field theory*, along with the Hartree–Fock approximation, which results in the wavefunctions being expressible as single Slater determinants of one electron orbitals [32,33]. The analogue of these orbitals in density functional theory are the Kohn–Sham orbitals, $\varphi_i(\mathbf{r})$, but it must be emphasised that if these are assembled into a Slater determinant they do not form eigenstates of a many particle Hamiltonian any more than do the Slater determinants in the Hartree–Fock theory. In both Hartree–Fock and density functional theory the electrons are described as *non-interacting* particles occupying one electron orbitals, $\varphi_i(\mathbf{r})$ and having one electron energy levels (eigenvalues) ε_i. One can construct an independent electron Green function

$$G(\mathbf{r}\mathbf{r}', \varepsilon) = \sum_i \frac{\varphi_i(\mathbf{r})\bar{\varphi}_i(\mathbf{r}')}{\varepsilon - \varepsilon_i}$$

similar to (A.11). As Hedin and Lundqvist explain [14], the effect of electron–electron interaction is that the *local* potential $V_{xc}(\mathbf{r})$ must be replaced by a non-local, energy-dependent potential known as the *self-energy operator* and denoted $\Sigma(\mathbf{r}\mathbf{r}', E)$. This describes in a non-average, dynamical way the effects of other electrons as an electron propagates in the electron gas. Electrons in this picture have a complex energy E, the real part is the quasiparticle energy, such as (A.9) and the Green function (A.11) is constructed from the more complex objects (A.10).

Hedin and Lundqvist [14] proposed an approximation to the self-energy which is now called the GW-approximation. The reason that the Hartree–Fock approximation is very poor in solids, especially metals, is that the exchange energy is the unscreened Coulomb interaction between the exchange charge. One should include screening of the Coulomb potential through a dynamically screened interaction W. The GW-approximation to the self-energy is $\Sigma = \mathrm{i}GW$. In many body language the GW-approximation amounts to a neglect of "vertex corrections". For complete details, see Aryasetiawan and Gunnarsson [34].

Appendix B. Density functional theory and the LMTO method

A very significant breakthrough in the understanding and implementation of electronic structure calculation was made in the mid-1960s when Hohenberg, Kohn and Sham showed that the many body problem of calculating total energy and electron density in the ground state can be reduced to a one-electron problem [11]. This is not the place to give full details; indeed the methods arising from DFT are now widely known [35]. However the salient facts are that the total energy of an electronic system in the ground state as a functional of the electron density $\rho(\mathbf{r})$ is the sum of three terms: the kinetic energy of a set of non-interacting fermions having the same density, the electrostatic self-energy of the charge distribution, including the positive charges of the nuclei and the "exchange and correlation" energy which accounts for the Pauli principle of antisymmetry of fermions (exchange) and dynamical correlations between electrons which are not accounted for by the average Hartree energy. The exchange and correlation energy also contains corrections to the kinetic energy to account for electron interactions. Hence all the many body parts of the problem are contained in the exchange and correlation energy; and this term has to be approximated to make a workable theory. The simplest, and most effective approach to this is to make the *local density approximation* (LDA) in which the functional is replaced pointwise in the electron gas by the function (which is known pretty accurately) for the

exchange and correlation energy of a uniform electron gas, taking the density of the gas as that which is encountered locally at each point. The total energy within DFT is written as

$$E[\rho] = T_s[\rho] + U[\rho] + E_{xc}[\rho], \tag{B.1}$$

which are the three terms described above. Kohn and Sham showed that without approximation the density and hence the total energy (and consequently force and stress) can be found by solving a one electron Schrödinger equation (or Kohn–Sham equation) for each electron

$$\left(-\frac{\hbar}{2m}\nabla^2 + V_{es}(\mathbf{r}) + V_{xc}(\mathbf{r})\right)\varphi_i(\mathbf{r}) = \varepsilon_i\varphi_i(\mathbf{r}). \tag{B.2}$$

The electrostatic potential energy is the electronic charge times the potential seen by an electron, namely

$$V_{es}(\mathbf{r}) = e^2\int \frac{\rho(\mathbf{r}')}{|\mathbf{r}-\mathbf{r}'|}\,\mathrm{d}\mathbf{r}' - e^2\sum_\nu \frac{Z_\nu}{|\mathbf{r}-\mathbf{R}_\nu|}. \tag{B.3}$$

Similarly, the potential energy seen by a nucleus is

$$V_\nu = e^2\sum_{\nu'\neq\nu}\frac{Z_\nu}{|\mathbf{R}_\nu - \mathbf{R}_{\nu'}|} - e^2\int\frac{\rho(\mathbf{r})}{|\mathbf{R}_\nu - \mathbf{r}|}.$$

Here, R_ν and Z_ν are the position and atomic number of nucleus ν. Formally, the "exchange and correlation potential" is the functional derivative,

$$V_{xc}(\mathbf{r}) = \frac{\delta E_{xc}}{\delta\rho}.$$

This functional and its derivative are unknown; but by making the local density approximation, the potential becomes

$$V_{xc}(\mathbf{r}) = \frac{\mathrm{d}}{\mathrm{d}\rho}(\rho\varepsilon_{xc}(\rho)),$$

where $\varepsilon_{xc}(\rho)$ is the exchange and correlation energy density of a uniform electron gas of density ρ. The point is that the density is represented as a sum over N Kohn–Sham orbitals:

$$\rho(\mathbf{r}) = \sum_{i=1}^{N}\overline{\varphi}_i(\mathbf{r})\varphi_i(\mathbf{r}), \tag{B.4}$$

and minimisation of (B.1) with respect to ρ leads directly to the Kohn–Sham Eq. (B.2), one for each orbital. The density functional method is tractable for computation and at the same time provides a transparent picture for the understanding of electronic structure. We all wish to view electronic processes in condensed matter with a non-interacting, or independent electron picture. This can now be done as long as we accept that the potential that goes into the Schrödinger equation is the "effective potential," $V_{\mathrm{eff}}(\mathbf{r}) = V_{es}(\mathbf{r}) + V_{xc}(\mathbf{r})$. There is, of course, a big price to pay; in reducing a many body problem to a single-particle picture, the resulting orbitals $\varphi_i(\mathbf{r})$ and their eigenenergies ε_i are strictly only mathematical constructs arising from the Euler–Lagrange minimisation of (B.1); these are very often interpreted as measurable electron states, but there is no rigorous justification for doing this. The present paper is, to a large extent, concerned with how such measurable electronic states and the transitions between them can be described within the local density approximation to density functional theory.

To calculate the total energy as a functional of the electron density, the electrostatic energy is written as

$$U[\rho] = \frac{1}{2}\int\rho(\mathbf{r})V_{es}(\mathbf{r}) + \frac{1}{2}\sum_\nu Z_\nu V_\nu.$$

From the Kohn–Sham equation (B.2) it follows that the kinetic energy of the non-interacting fermions belonging to the orbitals $\varphi_i(\mathbf{r})$ is

$$T_s[\rho] = \sum_{i=1}^{N}\varepsilon_i - \int\rho(\mathbf{r})V_{\mathrm{eff}}(\mathbf{r})\,\mathrm{d}\mathbf{r},$$

and the total energy in the LDA is conveniently written as

$$E[\rho] = \sum_{i=1}^{N}\varepsilon_i + \int\rho(\varepsilon_{xc} - V_{xc})\,\mathrm{d}\mathbf{r} - \frac{1}{2}\int\rho V_{es}\,\mathrm{d}\mathbf{r} + \frac{1}{2}\sum_\nu Z_\nu V_\nu.$$

It is now clear that the hard part of the problem is not the exchange and correlation, but the kinetic energy. To get the kinetic energy it is necessary to solve a *bandstructure* problem. This involves representing the Kohn–Sham orbitals and the charge density in suitable basis functions. This converts the Schrödinger equation (B.2) into a matrix eigenvalue problem which can be solved by numerical methods. The solution to (B.2) that minimises (B.1) must be found self-consistently, since the potential that enters the eigenproblem itself depends on the solution through equations (B.3) and (B.4).

There is also a spin density functional theory [36] which is the scheme that is used in the text to describe the electronic structure of CrN. The principal points are that the Kohn–Sham orbitals acquire a spin index which doubles the number of Kohn–Sham equations; V_{xc} becomes spin-dependent and the total energy depends on the charge density $\rho = \rho^\uparrow + \rho^\downarrow$ and the magnetic moment $m = \rho^\uparrow - \rho^\downarrow$.

The best known and most popular bandstructure scheme employs plane waves in the expansion of both the density and wavefunction [35]. In that case the nuclear potential in (B.3) is approximated by a pseudopotential and the core electrons are frozen in their atomic states. This approach is clearly not easily adaptable to the calculation of core level spectra by the inclusion of core holes. Generally the plane wave pseudopotential method is regarded as being the most efficient of the bandstructure schemes, but a recent method [15] based in the linear muffin-tin orbital (LMTO) approach is equally fast or faster on modern computers and has the advantage of being an "all electron" scheme in which the core electrons are explicitly retained. The valence electrons are represented in a basis of atom-centred atomic-like functions, $\chi_{\epsilon\mathbf{R}L}$ labelled

with a site index **R** angular momentum quantum numbers $L = \ell m$ and an additional energy variable ϵ:

$$\langle \mathbf{r}|n\mathbf{k}\rangle = \varphi_{n\mathbf{k}}(\mathbf{r}) = \sum_{\substack{n\mathbf{k}\\ \text{occ.}}} \sum_{\epsilon\mathbf{R}L} c_{n\mathbf{k},\epsilon\mathbf{R}L}\,\chi_{\epsilon\mathbf{R}L}. \tag{B.5}$$

The Kohn–Sham orbitals φ_i are labelled with n, the band index, and $\mathbf{k}$ the wavevector. The basis functions χ are "augmented smooth Hankel functions," this means that, in the spirit of Slater's augmented plane waves, space within the crystal is divided into spherical volumes about each atom (which may be overlapping) and the remaining "interstitial region." Atom-centred envelope functions are constructed around each atomic site. These are "smooth Hankel functions" that are close to Gaussian-like at the origin and have the asymptotic behaviour of a Hankel function of energy ϵ. The distance from the origin at which they are indistinguishable from a Hankel function is determined by a "smoothing radius" that is assigned to each envelope function. The envelopes are multiplied by real spherical harmonics [11] Y_L to give them atomic orbital like angular momentum. To arrive at a basis function, the envelopes are "augmented," that is replaced within each atomic sphere by solutions of the radial Schrödinger equation of angular momentum L and at a given energy ϵ_0 determined by the boundary conditions that the resulting wavefunctions should be continuous and differentiable everywhere. The radial Schrödinger equation is solved at each iteration toward self-consistency in each atomic sphere, so that the basis set is flexible, not fixed as in a conventional linear combination of atomic orbitals. Because the radial Schrödinger equation is solved for all electrons in the potential of the nucleus (and the Madelung potential of other nuclei) the core wavefunctions are also computed at each iteration and by construction are orthogonalised to the valence electrons. In the implementation used here, the core is assumed to be spherical and spin–orbit coupling is neglected; all other relativistic effects are included (Darwin and mass–velocity shifts). Complete details of the method have been recently published by Methfessel et al. [15].

In an augmented wave formulation of the bandstructure problem there is the simplification that for core level spectra we only need to know the expansion of the valence state $\langle \mathbf{r} \,|\, n\mathbf{k}\rangle$ *within a single atomic sphere*. This is because the matrix element that we seek involves integrating this state times the core wavefunction, and by definition the core wavefunction vanishes at the atomic sphere boundary. The LMTO method uses a construction for augmentation whereby functions $u_\ell(r)$ are defined which have the property that they have zero value at *each* sphere surface *except one*. Similarly functions $s_\ell(r)$ are constructed which have zero *slope* at each sphere surface except one [37]. These are then used in one centre expansions to enforce the values and slopes of the radial functions to ensure the matching boundary conditions at the sphere surfaces. Thereby the valence wavefunction is constructed from augmented envelopes centred at the site in question as well as augmented tails of envelopes centred at all other sites, which is what is meant by "one centre expansion." Hence an expansion analogous to the "$\phi\dot{\phi}$" expansion in conventional LMTO [38],

$$\begin{aligned}\langle \mathbf{r}|n\mathbf{k}\rangle &= \sum_L a^u_{n\mathbf{k},L} u_\ell(\mathbf{r}) Y_L(\mathbf{r}) + \sum_L a^s_{n\mathbf{k},L} s_\ell(\mathbf{r}) Y_L(\mathbf{r}) \\ &\equiv \sum_L f_{n\mathbf{k},L}(\mathbf{r}) Y_L(\mathbf{r}),\end{aligned}$$

is valid inside the atomic spheres. In order to calculate matrix elements of

$$\mathrm{e}^{\mathrm{i}\mathbf{q}\cdot\mathbf{r}} = 1 + \mathrm{i}\mathbf{q}\cdot\mathbf{r} - \tfrac{1}{2}(\mathbf{q}\cdot\mathbf{r})^2 + \cdots \tag{B.6}$$

between a core state $\langle \mathbf{r}|c_{\ell'}\rangle$ of angular momentum ℓ' (in this article we are confined to K-edges, for which $\ell' = 0$, we omit the index m' since we do not deal with multiplet effects), and a valence state $\langle n\mathbf{k} \,|\, \mathbf{r}\rangle$, we begin by writing real spherical harmonic polynomials [11]

$$R_L(\mathbf{r}) \equiv \sqrt{\frac{4\pi}{2\ell+1}} r^\ell Y_L(\mathbf{r}),$$

which can be used to express matrix elements of any power of $\mathbf{q}\cdot\mathbf{r}$ as a sum of radial integrals

$$\begin{aligned}M_{n\mathbf{k},L\ell'} &\equiv \langle n\mathbf{k}|R_L(\mathbf{r})|c_{\ell'}\rangle \\ &= \sqrt{\frac{4\pi}{2\ell+1}} \sum_{L''} C_{LL'L''} \int \bar{f}_{n\mathbf{k},L}(r) r^\ell c_{\ell'}(r) r^2\,\mathrm{d}r,\end{aligned}$$

where

$$C_{L''L'L} = \iint \mathrm{d}\Omega\, Y_{L''} Y_{L'} Y_L$$

are real Gaunt coefficients. It is these that take care of the selection rules; for example in the next equation these are zero unless $\ell'' = \ell' \pm 1$.

In the dipole approximation we have $\ell = 1$, and $\mathbf{q}\cdot\mathbf{r} = \sum_{m=1}^{3} R_{1m}(\mathbf{q}) R_{1m}(\mathbf{r})$, therefore

$$\langle n\mathbf{k}|\mathbf{q}\cdot\mathbf{r}|c_{\ell'}\rangle = \sqrt{\frac{4\pi}{3}} \sum_{L''} \sum_{mm'} q_m \langle f_{n\mathbf{k},L''}|r|c_{\ell'}\rangle C_{1m\ell'm'\ell''m''}.$$

Here [11], $R_{1m}(\mathbf{q}) = \{q_z, q_y, q_x\}$ and the radial integral

$$\langle f_{n\mathbf{k},L''}|r|c_{\ell'}\rangle = \int \bar{f}_{n\mathbf{k},L}(r) r \varphi_c(r) r^2\,\mathrm{d}r$$

can easily be done numerically. Since the Gaunt coefficients can be tabulated once and for all, the implementation of core level matrix elements into a full potential LMTO program can be done in a fairly straightforward way. In order to go beyond the dipole approximation, one uses the spherical harmonic polynomials of the second degree [11],

$$\begin{aligned}&R_{2m}(\mathbf{r}) = \\ &\{\tfrac{1}{2}(3r_3^2 - r^2)\ \ \sqrt{3}r_1r_3\ \ \sqrt{3}r_2r_3\ \ \tfrac{1}{2}\sqrt{3}(r_1^2 - r_2^2)\ \ \sqrt{3}r_1r_2\},\end{aligned}$$

whereby we find

$$\sum_m R_{2m}(\mathbf{q})R_{2m}(\mathbf{r}) = \frac{2}{3}(\mathbf{q}\cdot\mathbf{r})^2 - \frac{1}{2}(qr)^2$$

from which it follows that

$$\langle n\mathbf{k}|(\mathbf{q}\cdot\mathbf{r})^2|c_{\ell'}\rangle = \sqrt{\frac{9\pi}{5}}\sum_{L''}\sum_{mm'} \times R_{2m}(\mathbf{q})\langle f_{n\mathbf{k},L''}|r^2|c_{\ell'}\rangle C_{2m\ell'm'\ell''m''} + \frac{3}{4}q^2\sum_{m'}\langle f_{n\mathbf{k},L'}|r^2|c_{\ell'}\rangle.$$

In this way, if required, one can calculate matrix elements for a particular scattering vector **q**, if such a measurement can be made; and also add terms beyond the dipole approximation [39].

References

[1] G. Onida, L. Reining, A. Rubio, Rev. Mod. Phys. 74 (2002) 601.
[2] D.A. Muller, P.E. Batson, S. Subramanian, S.L. Sass, J. Silcox, Mater. Res. Soc. Symp. Proc. 319 (1994) 299.
[3] R.F. Klie, M. Beleggia, Y. Zhu, J.P. Buban, N.D. Browning, Phys. Rev. B 68 (2003) 214101.
[4] F. de Groot, Chem. Rev. 101 (2001) 1779.
[5] D.A. Muller, D.J. Singh, J. Silcox, Phys. Rev. B 57 (1998) 8181.
[6] A.T. Paxton, M. van Schilfgaarde, M. MacKenzie, A.J. Craven, J. Phys.: Condens. Matter 12 (2000) 729.
[7] L.I. Schiff, Quantum Mechanics, 3rd ed., McGraw-Hill, 1968.
[8] H. Bethe, Annalen der Physik. 5 (1930) 325.
[9] H.A. Bethe, Intermediate Quantum Mechanics, Benjamin, New York, 1964.
[10] D. Pines, P. Nozieres, The Theory of Quantum Liquids, vol. I: Normal Fermi Liquids, Benjamin, New York, 1966.
[11] M.W. Finnis, Interatomic Forces in Condensed Matter, Oxford University Press, Oxford, 2003 (Chapter 1).
[12] P. Roman, Advanced Quantum Theory, Addison-Wesley, Reading, MA, 1965.
[13] L. Hedin, Solid State Commun. 5 (1967) 451.
[14] L. Hedin, S. Lundqvist, Solid State Phys. 23 (1967) 1.
[15] M. Methfessel, M. van Schilfgaarde, R.A. Casali, in: H. Dreysse (Ed.), Electronic Structure and Physical Properties of Solids, Springer Verlag, Berlin, 2000.
[16] A.T. Paxton, A.J. Craven, J.M. Gregg, D. McComb, J. Microsc. 210 (2003) 35.
[17] L.M. Corliss, N. Elliot, J.M. Hastings, Phys. Rev. 117 (1960) 929.
[18] M. Nasr-Eddine, E.F. Bertaut, Solid State Commun. 9 (1971) 717.
[19] A. Filippetti, N.A. Hill, Phys. Rev. Lett. 85 (2000) 5166.
[20] D.W. McComb, A.J. Craven, L. Chioncel, A.I. Lichtenstein, F.T. Docherty, Phys. Rev. B 68 (2003) 224420.
[21] D.J. Singh, Phys. Rev. B 43 (1991) 6388.
[22] S. Fabris, A.T. Paxton, M.W. Finnis, Phys. Rev. B 61 (2000) 6617.
[23] D.W. McComb, Phys. Rev. B 54 (1996) 7094.
[24] S. Ostanin, A.J. Craven, D.W. McComb, D. Vlachos, A. Alavi, M.W. Finnis, A.T. Paxton, Phys. Rev. B 62 (2001) 14728.
[25] C. Elsasser, S. Kostlmeier, Ultramicroscopy 86 (2001) 325.
[26] K. Terakura, A.R. Williams, T. Oguchi, J. Kiibler, Phys. Rev. Lett. 52 (1984) 1830.
[27] G.A. Sawatzky, J.W. Allen, Phys. Rev. Lett. 53 (1984) 2339.
[28] J. Zaanen, G.A. Sawatzky, J.W. Allen, Phys. Rev. Lett. 55 (1985) 65.
[29] S.L. Dudarev, G.A. Botton, S.Y. Savrasov, C.J. Humphreys, A.P. Sutton, Phys. Rev. B 57 (1998) 1505.
[30] F. Aryasetiawan, O. Gunnarsson, Phys. Rev. Lett. 74 (1995) 3221.
[31] S.V. Faleev, M. van Schilfgaarde, T. Kotani, Phys. Rev. Lett. 93 (2004) 126406.
[32] H. Haken, Quantum Field Theory of Solids, North-Holland, Amsterdam, 1976.
[33] R.G. Parr, W. Yang, Density Functional Theory of Molecules and Solids, Oxford University Press, Oxford, 1989.
[34] F. Aryasetiawan, O. Gunnarsson, Rep. Prog. Phys. 61 (1998) 237.
[35] D.J. Singh, Planewaves, Pseudopotentials and the LAPW Method, Kluwer Academic Publishers, 1993.
[36] O. Gunnarsson, B.I. Lundqvist, Phys. Rev. B 13 (1976) 4274.
[37] M. Methfessel, Phys. Rev. B 38 (1988) 1537.
[38] O.K. Andersen, in: P. Phariseau, W.M. Temmerman (Eds.), The Electronic Structure of Complex Systems, Plenum Press, New York, 1984.
[39] M. Nelhiebel, P.-H. Louf, P. Schattschneider, P. Blaha, K. Schwarz, B. Jouffrey, Phys. Rev. B 59 (1999) 12807.